Dewetting of an Evaporating Thin Liquid Film: Heterogeneous Nucleation and Surface Instability

Uwe Thiele, Michael Mertig, and Wolfgang Pompe
Institut für Werkstoffwissenschaft, Technische Universität Dresden, D-01062 Dresden, Germany
(Received 13 November 1997)

Film rupture as the initial stage of dewetting is investigated for a volatile, spin-coated nonwetting film. During structure formation in the liquid film the film thickness is continuously reduced via evaporation. The dynamical character of the experiment allows the study of hole formation caused by distinct rupture mechanisms occurring at different film thicknesses. Both heterogeneous nucleation for thick films as well as spinodal dewetting for film thickness below 10 nm have been observed. The balance between both processes can be shifted by controlling the ambient humidity. The structures resulting from film rupture are quantified with respect to their different geometrical properties. For the first time we find that spinodal dewetting is caused by destabilizing polar interactions. [S0031-9007(98)05676-2]

PACS numbers: 68.15.+e, 68.45.–v, 68.55.–a

The wetting behavior of films is of central importance for thin film technology since it determines the homogeneity of thin films and coatings [1–3]. Controlled dewetting can be employed to pattern thin films on the nanometer scale as was recently demonstrated by the production of biomolecular coatings with a defined structure for medical applications via spin coating of protein solutions [4].

Investigations of thin nonvolatile liquid films on nonwetting substrates have shown that dewetting takes place in three successive phases: rupture of the film, growth of the holes resulting in the formation of a polygonal network of straight liquid rims, and the decay of rims via a Rayleigh instability. The growth dynamics of single holes is well understood [5], whereas the understanding of film rupture as the initial stage of dewetting remains insufficient. From theoretical considerations, two possible rupture mechanisms have been discussed [6]: first, heterogeneous hole nucleation due to defects in the liquid film [7], and, second, spontaneous rupture under the influence of long range molecular forces [8], known as spinodal dewetting. These forces can destabilize a thin film (thickness, $h < 100$ nm) by causing surface fluctuations to grow exponentially. Rupture takes place on a length scale corresponding to the wavelength of the surface undulation whose amplitude increases most rapidly. In the case of an apolar Lifshitz–van der Waals interaction, this wavelength scales with the square of the film thickness [8]. In addition, polar interactions may become significant for systems such as aqueous solutions at the smallest film thickness ($h < 10$ nm), either stabilizing or destabilizing the film [9].

Up to now, experimental investigations of film rupture exist only for apolar films. The system studied in most detail is polystyrene (PS) on silicon [1,10]. However, with regard to the two rupture mechanisms mentioned above the experimental observations hitherto present a conflicting picture. An observed h^{-4} dependence of the density of initially formed holes has been taken as evidence for film surface instability [1]. However, recent investigations on PS films show that the spatial separation of the holes is not correlated as would be expected for spontaneous rupture at the wavelength of the fastest growing mode [10]. A novel approach to gain insight into film rupture is to realize experimental conditions which assist the simultaneous occurrence of both rupture mechanisms, as reported recently for thin metal films on fused silica substrates after melting by a laser pulse [3]. In this case, the liquid metal dewets from the substrate within a small time window before the film resolidifies. In addition to large circular holes assigned to heterogeneous nucleation, the appearance of small holes with a characteristic wavelength proportional to h^2 has been observed, giving strong evidence of spinodal dewetting. The investigations of both PS and metal films have been carried out at a constant film thickness of $h >$ 10 nm, whereby this lower thickness limit arises from the requirement that the film should be homogeneous.

In this Letter, we report on a novel dynamical dewetting procedure whereby a spin-coated, nonwetting thin film of a volatile liquid on a solid substrate is continuously reduced in thickness by evaporation. Under the condition that the characteristic time constant for viscous processes is much smaller than that of evaporation, structure formation in the liquid film is dominated by dewetting and not by the evaporation itself. Here, while the general scenario of dewetting is the same as that mentioned above, the dewetting process competes with the ongoing thinning of the film, which is accompanied by a continuing hole formation.

In this way a superposition of structures is arrived at whose evolution is initiated at different film thicknesses. This dynamical dewetting scheme therefore possesses two advantages: first, it allows the simultaneous observation of both rupture mechanisms on one and the same sample, and, second, it enables for the first time the study of the structure development for films at $h < 10$ nm not

accessible before by any other technique. The evaporation speed of the solvent, controlled by its partial pressure allows control of the rate of film thinning in comparison to the characteristic times of both rupture and hole growth. In this way the balance between the different rupture mechanisms can be altered. The resulting film structures are visualized by a small quantity of macromolecules in the solvent that dry-in on the substrate and thus decorate the finally developed film structure.

The dewetting experiments were performed with a monomeric collagen solution (protein concentration: 0.2 mg/ml) in 0.1 M acetic acid (pH 3). In some cases the collagen monomers were denatured by warming the precursor solution to 50 °C for 30 min. Freshly cleaved highly oriented pyrolytic graphite (HOPG) has been used as the substrate (contact angle of the precursor, $\theta = 75°$). Collagen films with an initial thickness of about 10 μm were prepared by spin coating under controlled relative humidity between 0% and 90% at room temperature. The films dry within tens of seconds. The final film structures were examined by scanning force microscopy (SFM) operating in tapping mode using a NanoScope IIIa (Digital Instruments). In comparable experiments with a very low protein concentration on mica, immobilized single collagen molecules with a diameter of 1.5 nm and a length of 300 nm could be imaged [4], indicating that the monomers are not damaged during sample preparation.

Figure 1 (left part) shows a series of SFM images of collagen films prepared under different ambient humidity conditions. A transition from structures consisting of some large, quasicircular holes embedded in a homogeneous pattern of very small holes [Fig. 1(a)] towards fully developed homogeneous polygonal networks [Fig. 1(d)] is observed with increasing humidity. To quantify the patterns, the distribution functions corresponding to the area occupied by holes belonging to a certain class of hole diameters (HDF) have been calculated and plotted in the right part of Fig. 1. We have chosen this particular representation, where the distribution function corresponds to the product of number of holes per class multiplied by the average area of the class, in order to evaluate the relative contributions of a limited number of larger holes in a background of numerous small holes. At 15% humidity the HDF exhibits two well separated peaks at 50 and 400 nm. The position of the second peak shifts steadily to larger diameters with increasing humidity. At the same time the height of the rims around the larger holes increases from about 3 to about 8 nm (not shown). Both the increasing diameter of the holes and the heightening of the accumulated material along their perimeter indicate that the time the large holes have to grow increases with increasing humidity. In contrast, the position of the first peak at 50 nm does not depend on humidity. However, it does vanish with increasing humidity.

The pronounced bimodality of the HDF at low humidity clearly indicates the occurrence of two distinct hole

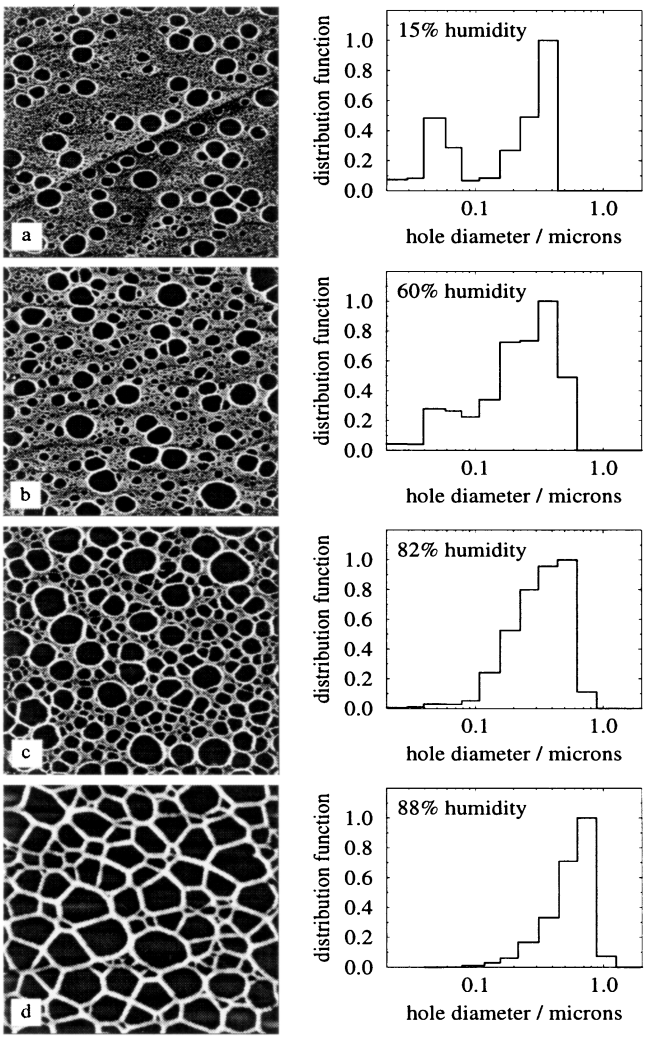

FIG. 1. Series of images of collagen films prepared at different humidities: (a) 15%, (b) 60%, (c) 82%, and (d) 88%. Left: SFM images (5 μm $\times$ 5 μm) in height mode. Right: Corresponding area weighted diameter distribution functions (in arbitrary units).

formation mechanisms. In particular, the completely different dependencies of the distributions of the larger and smaller holes on humidity, as well as the entire suppression of smaller holes at higher humidity suggest that the two hole types emerge at different film thicknesses. We assign the larger holes to film rupture due to heterogeneous nucleation at defects. Step lines between neighboring monolayer terraces of the HOPG are a probable defect source. This is supported by the observation that larger holes accumulate in the vicinity of these step lines when the step height is of the order of a few monolayer distances. On the contrary, we assign the 50 nm diameter holes to spinodal dewetting caused by destabilizing polar interactions. These interactions control the structure formation at film thicknesses below 10 nm. As is analyzed later on in more detail, in the present case the apolar

interactions stabilize the film, which would lead to the observed deep minimum between the two peaks in the HDF at low humidity.

The hypothesis that the film rupture mechanisms discussed above take place at different film thicknesses is strongly supported by the observation that the balance between the different predominant mechanisms can be varied by altering the ambient humidity. At high humidity the evaporation rate of the precursor solution is low. Thus, early in the process of film rupture nucleated holes have time to grow until neighboring holes meet and form common rims of polygonal networks as seen in Fig. 1(d). With decreasing humidity the time being available for hole growth reduces whereby the film structure yields to holes with smaller diameters. Consequently, the holes become increasingly isolated, and the area occupied by these holes decreases. That is, at high humidity heterogeneously nucleated holes may conquer the whole area before the remaining film gets thinner than 10 nm. In this case the formation of additional holes by spinodal dewetting cannot take place. If, however, nonruptured area remains when the thickness reaches the range where the destabilizing polar interactions become dominant, the film ruptures at once due to spinodal dewetting leading to the bimodal film patterns as observed at humidity below 70% [see Figs. 1(a) and 1(b)].

In the case, in which the thin film undergoes spinodal dewetting at the wavelength of the fastest growing mode, one expects a well developed short range order in the spatial hole distribution. To prove this, we have calculated the pair correlation function of the mass centers of all holes (PCF). Figure 2 shows the PCF of a sample prepared at 15% humidity. The PCF exhibits a pronounced maximum at $r_0 = 50$ nm. Further peaks are obtained at about $2 \times r_0$ and $3 \times r_0$. This result is in agreement with the value derived from the first maximum of the HDF [see Fig. 1(a)].

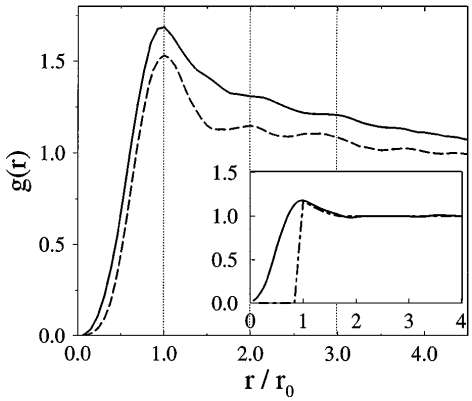

FIG. 2. Pair correlation functions of the mass centers of the holes of the same sample as shown in Fig. 1(a) (solid line) and of denatured collagen (dashed line). In the inset the correlation functions of the sample shown in Fig. 1(c) (solid line) and of a model hard-core Poisson distribution (dash-dotted line) are plotted. The corresponding r_0 values are given in the text.

Again, to make the difference between smaller and larger holes evident, we have calculated the PCF for the sample shown in Fig. 1(c) (82% humidity), where hole formation is dominated by heterogeneous nucleation. The result is plotted in the inset of Fig. 2. Here, the PCF exhibits only one less pronounced peak at $r_0' = 156$ nm. It decreases continuously for $r > r_0'$, quickly approaching $g(r) = 1$. This behavior can be reproduced by modeling the PCF of a hard-core Poisson distribution of points [11], drawn as a dotted line in the inset. The observed discrepancy at $r < r_0'$ can be explained by the fact that a "soft-core" [12] rather than a hard-core hole distribution is obtained in a dynamical dewetting experiment, resulting from a decrease of the critical hole nucleation radius caused by the decreasing thickness of the evaporating film.

Since the characteristic sizes of the observed film patterns have been found to be of the same order as the length of the collagen molecule used to decorate the developed film structures, it seems possible that the film structure formation itself might be influenced by the presence of collagen in the precursor. If this were the case, one would expect the largest effects for the surface instability because the observed wavelength for this process is much smaller than 300 nm. To investigate this, all of the above experiments have been repeated with denatured collagen. The size of the macromolecule decreases due to the change of the conformation into a random coil accompanied by a reduction of the mechanical stiffness of the molecule. We did not observe general differences in the experiments between the two collagen specimens, indicating that the observed structure formation is an intrinsic property of the solvent (water) HOPG system. The first peak of the PCF of denatured collagen prepared at 15% humidity (Fig. 2, dashed line) is observed at 53 nm. Thus, rupture of the films due to the surface instability takes place at very similar characteristic wavelengths in both collagen specimens, proving that the size of the molecules does not directly influence the hole formation process. However, as indicated by a larger ratio of the amplitude of the first maximum to the amplitude of the first minimum in the PCF, the structure of the denatured films appears more developed, as larger amplitude ratios are usually taken as a sign for a more pronounced pair correlation [12]. This result follows as a direct consequence of the reduced mechanical stiffness of the denatured collagen molecule—allowing the molecule to follow movements of the solvent on the substrate during structure formation more easily. However, we never observed coalescence of holes, which is a result of the stabilization of the rims by the collagen molecules. Structure stabilization is one of the advantages of the method of dynamical dewetting described here, since it allows the observation of features generated in the early stages of film formation.

The appearance of a surface instability in thin films can be described by hydrodynamics within the lubrication approximation of the Stokes equation under consideration

of long range molecular interactions [8]. The time evolution of the film thickness can be derived from the partial differential equation, $h_t = -(h^3/3\eta(\gamma h_{xx} + \Pi(h))_x)_x$, where subscripts x and t denote spatial and time derivatives, respectively, η is the effective viscosity, γ is the surface tension, and $\Pi(h)$ is the thickness-dependent disjoining pressure [7,13]. A linear stability analysis yields the wavelength of the fastest growing mode, $\lambda = 2\pi\sqrt{2\gamma(d\Pi/dh)^{-1}}$, and its typical rupture time, $\tau = 6\eta\gamma/h^3(d\Pi/dh)^{-2}$. λ only exhibits nonimaginary values if the argument of the square root is positive. That is, the film is unstable for $d\Pi/dh \geq 0$ and stable otherwise. The disjoining pressure containing the polar and apolar interaction contributions is given by [9]

$$\Pi(h) = 2S_{AP}\frac{d_0^2}{h^3} + \frac{S_P}{l}e^{[(d_0-h)/l]}. \quad (1)$$

Here $d_0 = 0.158$ nm is the Born repulsion length, and l is the correlation length of a polar fluid. For water, l is approximately 0.6 nm [9]. S_P and S_{AP} are the polar and apolar components of the total spreading coefficient, $S = S_{AP} + S_P = \gamma(\cos\theta - 1)$, where θ is the macroscopic contact angle. From Eq. (1) it can be seen that film rupture due to surface instability may only occur if at least one component of S is negative. The apolar component S_{AP} is derived from the effective Hamaker constant A of the air–thin film–substrate system, $S_{AP} = -A/12\pi d_0^2$, where A can be calculated from the individual constants of water (W) and graphite (G) by the sum rules: $A = A_{WW} - A_{GW} \approx \sqrt{A_{WW}}(\sqrt{A_{WW}} - \sqrt{A_{GG}})$ [13,14]. Applying this formalism to the system water on graphite studied here ($\theta = 75°$, $\gamma = 72.2 \times 10^{-3}$ N/m, $A_{WW} = 4.38 \times 10^{-20}$ N m, $A_{GG} = 47.0 \times 10^{-20}$ N m [15]) yields $S = -53 \times 10^{-3}$ N/m, $S_{AP} = 106 \times 10^{-3}$ N/m, and $S_P = -159 \times 10^{-3}$ N/m. Consequently, the apolar part of the interaction acts stabilizing, whereas the polar contribution destabilizes the film. The polar interaction becomes dominating for $h < h_C$, where h_C can be calculated from Eq. (1) under the condition $d\Pi/dh = 0$. For l between 0.5 and 0.8 nm h_C is between 5 and 10 nm.

The driving force grows exponentially with decreasing film thickness $h < h_C$, leading to exponential decrease of both τ and λ. Thus, τ may become much smaller than the typical evaporation time, yielding to spontaneous rupture of the remaining film. However, to give an estimate of the rupture time, one has to make a realistic assumption for the viscosity of the solution, which might become very high for the last stages of solvent evaporation and can, unfortunately, not be directly measured for those high collagen concentrations. On the other hand, due to the exponential dependency of Eq. (1), a realistic estimate of the lower bound of viscosity will already yield a good assessment of the rupture time. Assuming $\eta \approx 1000$ Pa s (derived by an extrapolation from low concentration data [16]), τ becomes smaller than the evaporation time of the remaining liquid, which is typically of the order of tenths of a second, at a film thickness between 2 and 6 nm. With these values the corresponding wavelength of the instability can be estimated to be between 20 and 80 nm, respectively. This is in good agreement with the observed value of 50 nm.

In conclusion, in dynamical dewetting experiments we have observed two coexisting film rupture mechanisms occurring at different film thicknesses down to below 10 nm. The film structures exhibit distinct spatial order: holes initiated by heterogeneous nucleation at defects are randomly distributed, whereas holes resulting from spinodal dewetting exhibit a well developed short range order with a periodicity that corresponds to the calculated value taking polar interactions into consideration.

We wish to thank J. Bradt, D. Klemm, and H. Wendrock for assistance in the experiments and geometrical analysis of film structures. We thank P. Leiderer for valuable discussions and M. S. Golden for a critical reading of the manuscript.

[1] G. Reiter, Phys. Rev. Lett. **68**, 75 (1992).
[2] R. Yerushalmi-Rozen, J. Klein, and L. J. Fetters, Science **263**, 793 (1994).
[3] J. Bischof *et al.*, Phys. Rev. Lett. **77**, 1536 (1996).
[4] M. Mertig *et al.*, Surf. Interface Anal. **25**, 514 (1997).
[5] C. Redon, F. Brochard-Wyart, and F. Rondelez, Phys. Rev. Lett. **66**, 715 (1991).
[6] F. Brochard-Wyart and J. Daillant, Can. J. Phys. **68**, 1084 (1989).
[7] H. S. Kheshgi and L. E. Scriven, Chem. Eng. Sci. **46**, 519 (1991).
[8] E. Ruckenstein and R. K. Jain, J. Chem. Soc. Faraday Trans. II **70**, 132 (1974).
[9] A. Sharma, Langmuir **9**, 861 (1993).
[10] K. Jacobs, S. Herminghaus, and K. R. Mecke (to be published).
[11] H. Hermann, *Stochastic Models of Heterogeneous Materials* (Trans Tech Publications Ltd., Zürich, 1991).
[12] D. Stoyan and H. Stoyan, *Fraktale-Formen-Punktfelder* (Akademie Verlag, Berlin, 1992).
[13] J. N. Israelachvili, *Intermolecular and Surface Forces* (Academic Press, London, 1992).
[14] R. J. Hunter, *Foundation of Colloid Science* (Clarendon Press, Oxford, 1992), Vol. 1.
[15] J. Visser, Adv. Colloid Interface Sci. **3**, 331 (1972).
[16] J.-C. Ronzon, Collagen Rel. Res. **7**, 201 (1987).